Fast Texture Synthesis using Tree-structured Vector Quantization

Li-Yi Wei Marc Levoy

Stanford University *

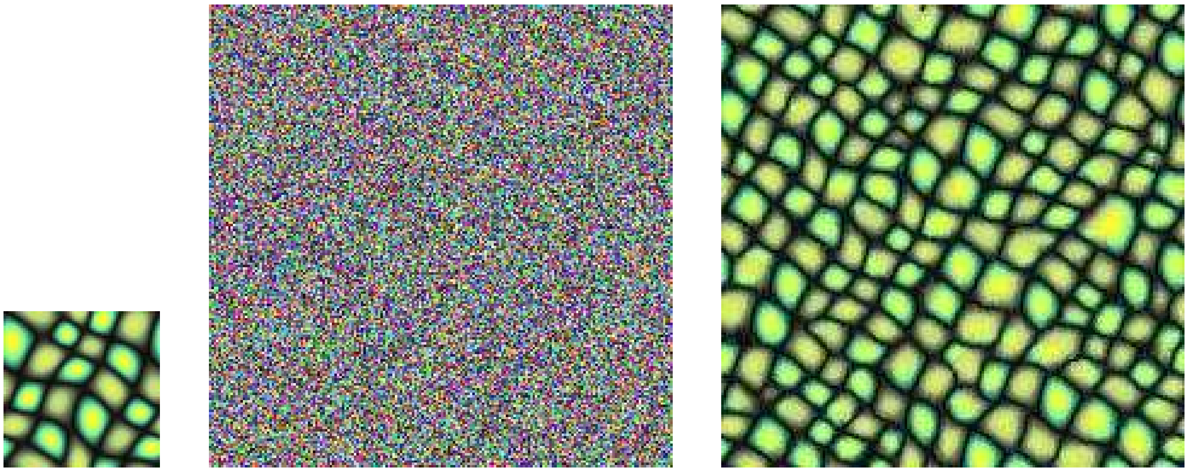

Figure 1: *Our texture generation process takes an example texture patch (left) and a random noise (middle) as input, and modifies this random noise to make it look like the given example texture. The synthesized texture (right) can be of arbitrary size, and is perceived as very similar to the given example. Using our algorithm, textures can be generated within seconds, and the synthesized results are always tileable.*

Abstract

Texture synthesis is important for many applications in computer graphics, vision, and image processing. However, it remains difficult to design an algorithm that is both efficient and capable of generating high quality results. In this paper, we present an efficient algorithm for realistic texture synthesis. The algorithm is easy to use and requires only a sample texture as input. It generates textures with perceived quality equal to or better than those produced by previous techniques, but runs two orders of magnitude faster. This permits us to apply texture synthesis to problems where it has traditionally been considered impractical. In particular, we have applied it to constrained synthesis for image editing and temporal texture generation. Our algorithm is derived from Markov Random Field texture models and generates textures through a deterministic searching process. We accelerate this synthesis process using tree-structured vector quantization.

*Gates Computer Science Building, Stanford, CA 94305
Email: {liyiwei | levoy}@graphics.stanford.edu
WWW: http://graphics.stanford.edu/projects/texture/

Keywords: Texture Synthesis, Compression Algorithms, Image Processing

1 Introduction

Texture is a ubiquitous visual experience. It can describe a wide variety of surface characteristics such as terrain, plants, minerals, fur and skin. Since reproducing the visual realism of the physical world is a major goal for computer graphics, textures are commonly employed when rendering synthetic images. These textures can be obtained from a variety of sources such as hand-drawn pictures or scanned photographs. Hand-drawn pictures can be aesthetically pleasing, but it is hard to make them photo-realistic. Most scanned images, however, are of inadequate size and can lead to visible seams or repetition if they are directly used for texture mapping.

Texture synthesis is an alternative way to create textures. Because synthetic textures can be made any size, visual repetition is avoided. Texture synthesis can also produce tileable images by properly handling the boundary conditions. Potential applications of texture synthesis are also broad; some examples are image denoising, occlusion fill-in, and compression.

The goal of texture synthesis can be stated as follows: Given a texture sample, synthesize a new texture that, when perceived by a human observer, appears to be generated by the same underlying stochastic process. The major challenges are 1) modeling- how to estimate the stochastic process from a given finite texture sample and 2) sampling- how to develop an efficient sampling procedure to produce new textures from a given model. Both the modeling and sampling parts are essential for the success of texture synthesis: the visual fidelity of generated textures will depend primarily on the accuracy of the modeling, while the efficiency of the sampling procedure will directly determine the computational cost of texture generation.

In this paper, we present a very simple algorithm that can efficiently synthesize a wide variety of textures. The inputs consist of an example texture patch and a random noise image with size specified by the user (Figure 1). The algorithm modifies this random noise to make it look like the given example. This technique is flexible and easy to use, since only an example texture patch (usually a photograph) is required. New textures can be generated with little computation time, and their tileability is guaranteed. The algorithm is also easy to implement; the two major components are a multiresolution pyramid and a simple searching algorithm.

The key advantages of this algorithm are quality and speed: the quality of the synthesized textures are equal to or better than those generated by previous techniques, while the computation speed is two orders of magnitude faster than those approaches that generate comparable results to our algorithm. This permits us to apply our algorithm in areas where texture synthesis has traditionally been considered too expensive. In particular, we have extended the algorithm to constrained synthesis for image editing and motion texture synthesis.

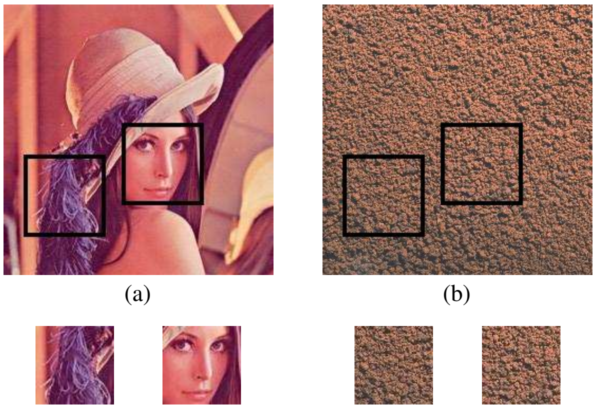

Figure 2: *How textures differ from images. (a) is a general image while (b) is a texture. A movable window with two different positions are drawn as black squares in (a) and (b), with the corresponding contents shown below. Different regions of a texture are always perceived to be similar (b1,b2), which is not the case for a general image (a1,a2). In addition, each pixel in (b) is only related to a small set of neighboring pixels. These two characteristics are called stationarity and locality, respectively.*

1.1 Previous Work

Numerous approaches have been proposed for texture analysis and synthesis, and an exhaustive survey is beyond the scope of this paper. We briefly review some recent and representative works and refer the reader to [8] and [12] for more complete surveys.

Physical Simulation: It is possible to synthesize certain surface textures by directly simulating their physical generation processes. Biological patterns such as fur, scales, and skin can be modeled using reaction diffusion [26] and cellular texturing [27]. Some weathering and mineral phenomena can be faithfully reproduced by detailed simulations [5]. These techniques can produce textures directly on 3D meshes so the texture mapping distortion problem is avoided. However, different textures are usually generated by very different physical processes so these approaches are applicable to only limited classes of textures.

Markov Random Field and Gibbs Sampling: Many algorithms model textures by Markov Random Fields (or in a different mathematical form, Gibbs Sampling), and generate textures by probability sampling [6, 28, 20, 18]. Since Markov Random Fields have been proven to be a good approximation for a broad range of textures, these algorithms are general and some of them produce good results. A drawback of Markov Random Field sampling, though, is that it is computationally expensive: even small texture patches can take hours or days to generate.

Feature Matching: Some algorithms model textures as a set of features, and generate new images by matching the features in an example texture [9, 4, 22]. These algorithms are usually more efficient than Markov Random Field algorithms. Heeger and Bergen [9] model textures by matching marginal histograms of image pyramids. Their technique succeeds on highly stochastic textures but fails on more structured ones. De Bonet [4] synthesizes new images by randomizing an input texture sample while preserving the cross-scale dependencies. This method works better than [9] on structured textures, but it can produce boundary artifacts if the input texture is not tileable. Simoncelli and Portilla [22] generate textures by matching the joint statistics of the image pyramids. Their method can successfully capture global textural structures but fails to preserve local patterns.

1.2 Overview

Our goal was to develop an algorithm that combines the advantages of previous approaches. We want it to be efficient, general, and able to produce high quality, tileable textures. It should also be user friendly; i.e., the number of tunable input parameters should be minimal. This can be achieved by a careful selection of the texture modeling and synthesis procedure. For the texture model, we use Markov Random Fields (MRF) since they have been proven to cover the widest variety of useful texture types. To avoid the usual computational expense of MRFs, we have developed a synthesis procedure which avoids explicit probability construction and sampling.

Markov Random Field methods model a texture as a realization of a *local* and *stationary* random process. That is, each pixel of a texture image is characterized by a small set of spatially neighboring pixels, and this characterization is the same for all pixels. The intuition behind this model can be demonstrated by the following experiment (Figure 2). Imagine that a viewer is given an image, but only allowed to observe it through a small movable window. As the window is moved the viewer can observe different parts of the image. The image is stationary if, under a proper window size, the observable portion always appears similar. The image is local if each pixel is predictable from a small set of neighboring pixels and is independent of the rest of the image.

Based on these locality and stationarity assumptions, our algorithm synthesizes a new texture so that it is locally similar to an example texture patch. The new texture is generated pixel by pixel, and each pixel is determined so that local similarity is preserved between the example texture and the result image. This synthesis procedure, unlike most MRF based algorithms, is completely deterministic and no explicit probability distribution is constructed. As a result, it is efficient and amenable to further acceleration.

The remainder of the paper is organized as follows. In Section 2, we present the algorithm. In Section 3, we demonstrate synthesis results and compare them with those generated by previous approaches. In Section 4, we propose acceleration techniques. In Sections 5 and 6, we discuss applications, limitations, and extensions.

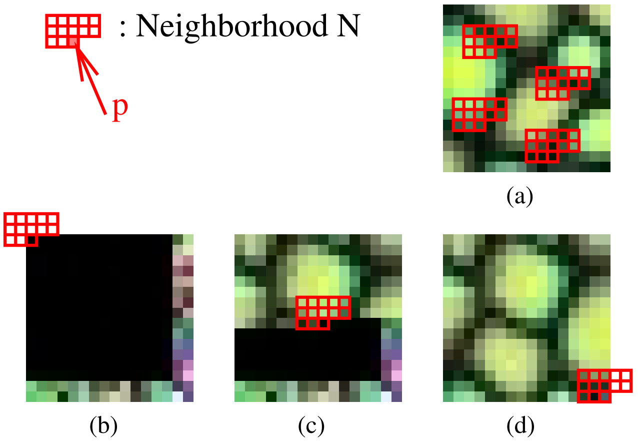

Figure 3: *Single resolution texture synthesis. (a) is the input texture and (b)-(d) show different synthesis stages of the output image. Pixels in the output image are assigned in a raster scan ordering. The value of each output pixel p is determined by comparing its spatial neighborhood $N(p)$ with all neighborhoods in the input texture. The input pixel with the most similar neighborhood will be assigned to the corresponding output pixel. Neighborhoods crossing the output image boundaries (shown in (b) and (d)) are handled toroidally, as discussed in Section 2.4. Although the output image starts as a random noise, only the last few rows and columns of the noise are actually used. For clarity, we present the unused noise pixels as black. (b) synthesizing the first pixel, (c) synthesizing the middle pixel, (d) synthesizing the last pixel.*

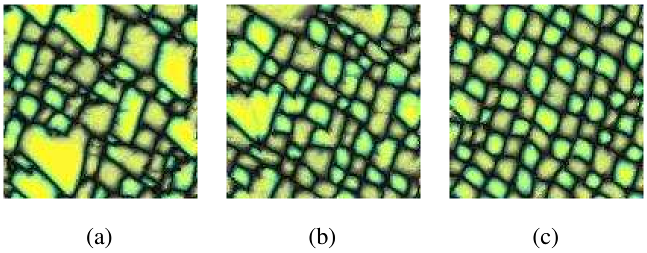

Figure 4: *Synthesis results with different neighborhood sizes. The neighborhood sizes are (a) 5x5, (b) 7x7, (c) 9x9, respectively. All images shown are of size 128x128. Note that as the neighborhood size increases the resulting texture quality gets better. However, the computation cost also increases.*

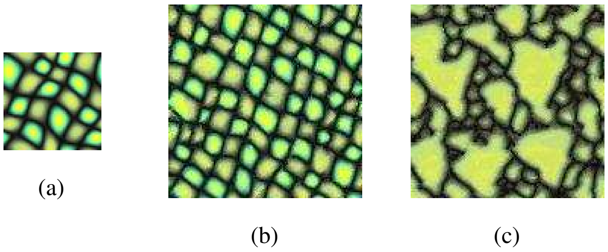

Figure 5: *Causality of the neighborhood. (a) sample texture (b) synthesis result using a causal neighborhood (c) synthesis result using a noncausal neighborhood. Both (b) and (c) are generated from the same random noise using a 9x9 neighborhood. As shown, a noncausal neighborhood is unable to generate valid results.*

2 Algorithm

Using Markov Random Fields as the texture model, the goal of the synthesis algorithm is to generate a new texture so that each local region of it is similar to another region from the input texture. We first describe how the algorithm works in a single resolution, and then we extend it using a multiresolution pyramid to obtain improvements in efficiency. For easy reference, we list the symbols used in Table 1 and summarize the algorithm in Table 2.

Symbol	Meaning
I_a	Input texture sample
I_s	Output texture image
G_a	Gaussian pyramid built from I_a
G_s	Gaussian pyramid built from I_s
p_i	An input pixel in I_a or G_a
p	An output pixel in I_s or G_s
$N(p)$	Neighborhood around the pixel p
$G(L)$	Lth level of pyramid G
$G(L, x, y)$	Pixel at level L and position (x, y) of G
{RxC,k}	(2D) neighborhood containing k levels, with size RxC at the top level
{RxCxD,k}	3D neighborhood containing k levels, with size RxCxD at the top level

Table 1: *Table of symbols*

2.1 Single Resolution Synthesis

The algorithm starts with an input texture sample I_a and a white random noise I_s. We force the random noise I_s to look like I_a by transforming I_s pixel by pixel in a raster scan ordering, i.e. from top to bottom and left to right. Figure 3 shows a graphical illustration of the synthesis process.

To determine the pixel value p at I_s, its spatial neighborhood $N(p)$ (the L-shaped regions in Figure 3) is compared against all possible neighborhoods $N(p_i)$ from I_a. The input pixel p_i with the most similar $N(p_i)$ is assigned to p. We use a simple L_2 norm (sum of squared difference) to measure the similarity between the neighborhoods. The goal of this synthesis process is to ensure that the newly assigned pixel p will maintain as much local similarity between I_a and I_s as possible. The same process is repeated for each output pixel until all the pixels are determined. This is akin to putting together a jigsaw puzzle: the pieces are the individual pixels and the fitness between these pieces is determined by the colors of the surrounding neighborhood pixels.

2.2 Neighborhood

Because the set of local neighborhoods $N(p_i)$ is used as the primary model for textures, the quality of the synthesized results will depend on its size and shape. Intuitively, the size of the neighborhoods should be on the scale of the largest regular texture structure; otherwise this structure may be lost and the result image will look too random. Figure 4 demonstrates the effect of the neighborhood size on the synthesis results.

The shape of the neighborhood will directly determine the quality of I_s. It must be causal, i.e. the neighborhood can only contain those pixels preceding the current output pixel in the raster scan ordering. The reason is to ensure that each output neighborhood $N(p)$ will include only already assigned pixels. For the first few rows and columns of I_s, $N(p)$ may contain unassigned (noise) pixels but as the algorithm progresses all the other $N(p)$ will be completely "valid" (containing only already assigned pixels). A non-

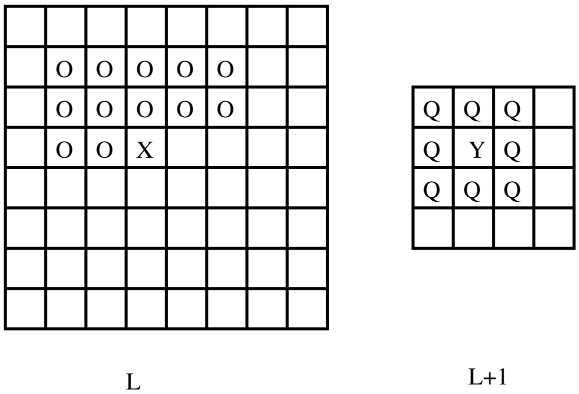

Figure 6: *A causal multiresolution neighborhood with size {5x5,2}. The current level of the pyramid is shown at left and the next lower resolution level is shown at right. The current output pixel p, marked as X, is located at (L, x, y), where L is the current level number and (x, y) is its coordinate. At this level L of the pyramid the image is only partially complete. Thus, we must use the preceding pixels in the raster scan ordering (marked as O). The position of the parent of the current pixel, located at $(L+1, \frac{x}{2}, \frac{y}{2})$, is marked as Y. Since the parent's level is complete, the neighborhood can contain pixels around Y, marked by Q. When searching for a match for pixel X, the neighborhood vector is constructed that includes the O's, Q's, and Y, in scanline order.*

causal $N(p)$, which always includes unassigned pixels, is unable to transform I_s to look like I_a (Figure 5). Thus, the noise image is only used when generating the first few rows and columns of the output image. After this, it is ignored.

2.3 Multiresolution Synthesis

The single resolution algorithm captures the texture structures by using adequately sized neighborhoods. However, for textures containing large scale structures we have to use large neighborhoods, and large neighborhoods demand more computation. This problem can be solved by using a multiresolution image pyramid [3]; computation is saved because we can represent large scale structures more compactly by a few pixels in a certain lower resolution pyramid level.

The multiresolution synthesis algorithm proceeds as follows. Two Gaussian pyramids, G_a and G_s, are first built from I_a and I_s, respectively. The algorithm then transforms G_s from lower to higher resolutions, such that each higher resolution level is constructed from the already synthesized lower resolution levels. This is similar to the sequence in which a picture is painted: long and thick strokes are placed first, and details are then added. Within each output pyramid level $G_s(L)$, the pixels are synthesized in a way similar to the single resolution case where the pixels are assigned in a raster scan ordering. The only modification is that for the multiresoltion case, each neighborhood $N(p)$ contains pixels in the current resolution as well as those in the lower resolutions. The similarity between two multiresolution neighborhoods is measured by computing the sum of the squared distance of all pixels within them. These lower resolution pixels constrain the synthesis process so that the added high frequency details will be consistent with the already synthesized low frequency structures.

An example of a multiresolution neighborhood is shown in Figure 6. It consists of two levels, with sizes 5x5 and 3x3, respectively. Within a neighborhood, we choose the sizes of the lower levels so that they are about half the sizes of the previous higher resolution levels. For clarity, we use the symbol {RxC,k} to indicate multiresolution neighborhoods which contain k levels with size RxC at the top level.

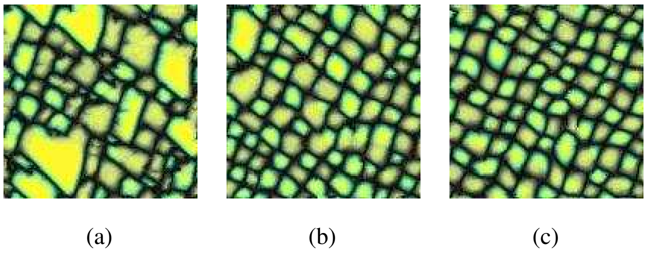

Figure 7: *Synthesis results with the same neighborhood, but different numbers of pyramid levels (a) 1 level, (b) 2 levels, (c) 3 levels. Except for the lowest resolution, which is synthesized with a 5x5 single resolution neighborhood, each pyramid level is synthesized using the multiresolution neighborhood shown in Figure 6. Note that as the number of pyramid levels increases, the image quality improves.*

Figure 7 shows results of multiresolution synthesis with different numbers of pyramid levels. Note that Figure 7 (c), although synthesized with a small {5x5,2} multiresolution neighborhood, looks comparable with Figure 4 (c), which was generated with a larger 9x9 single resolution neighborhood. This demonstrates a major advantage of multiresolution synthesis: moderately small neighborhoods can be used without sacrificing synthesis qualities.

2.4 Edge Handling

Proper edge handling for $N(p)$ near the image boundaries is very important. For the synthesis pyramid the edge is treated toroidally. In other words, if $G_s(L, x, y)$ denotes the pixel at level L and position (x, y) of pyramid G_s, then $G_s(L, x, y) \equiv G_s(L,\ x\ mod\ M,\ y\ mod\ N)$, where M and N are the number of rows and columns, respectively, of $G_s(L)$. Handling edges toroidally is essential to guarantee that the resulting synthetic texture will tile seamlessly. [1]

For the input pyramid G_a, toroidal neighborhoods typically contain discontinuities unless I_a is tileable. A reasonable edge handler for G_a is to pad it with a reflected copy of itself. Another solution is to use only those $N(p_i)$ completely inside G_a, and discard those crossing the boundaries. Because a reflective edge handler may introduce discontinuities in the derivative, we adopt the second solution which uses only interior blocks.

2.5 Initialization

Natural textures often contain recognizable structures as well as a certain amount of randomness. Since our goal is to reproduce realistic textures, it is essential that the algorithm capture the random aspect of the textures. This notion of randomness can sometimes be achieved by entropy maximization [28], but the computational cost is prohibitive. Instead, we initialize the output image I_s as a white random noise, and gradually modify this noise to look like the input texture I_a. This initialization step seeds the algorithm with sufficient entropy, and lets the rest of the synthesis process focus on the transformation of I_s towards I_a. To make this random noise a better initial guess, we also equalize the pyramid histogram of G_s with respect to G_a [9].

[1] The multiresolution algorithm is also essential for tileability if a causal neighborhood is used. Since a single resolution causal neighborhood $N(p)$ contains only pixels above p in scanline order, the vertical tileability may not be enforced. A multiresolution neighborhood, which contains symmetric regions at lower resolution levels, avoids this problem.

The initial noise affects the synthesis process in the following way. For the single resolution case, neighborhoods in the first few rows and columns of I_s contain noise pixels. These noise pixels introduce uncertainty in the neighborhood matching process, causing the boundary pixels to be assigned semi-stochastically (However, the searching process is still deterministic. The randomness is caused by the initial noise). The rest of the noise pixels are overwritten directly during synthesis. For the multiresolution case, however, more of the noise pixels contribute to the synthesis process, at least indirectly, since they determine the initial value of the lowest resolution level of G_s.

2.6 Summary of Algorithm

We summarize the algorithm in the following pseudocode.

function $I_s \leftarrow$ TextureSynthesis(I_a, $outputSize$)

1 $I_s \leftarrow$ Initialize($outputSize$);
2 $G_a \leftarrow$ BuildPyramid(I_a);
3 $G_s \leftarrow$ BuildPyramid(I_s);
4 **foreach** level L from lower to higher resolutions of G_s
5   **loop** through all pixels (x_s, y_s) of $G_s(L)$
6         $C \leftarrow$ FindBestMatch(G_a, G_s, L, x_s, y_s);
7         $G_s(L, x_s, y_s) \leftarrow C$;
8 $I_s \leftarrow$ ReconPyramid(G_s);
9 **return** I_s;

function $C \leftarrow$ FindBestMatch(G_a, G_s, L, x_s, y_s)

1 $N_s \leftarrow$ BuildNeighborhood(G_s, L, x_s, y_s);
2 $N_a^{best} \leftarrow$ null; $C \leftarrow$ null;
3 **loop** through all pixels (x_a, y_a) of $G_a(L)$
4     $N_a \leftarrow$ BuildNeighborhood(G_a, L, x_a, y_a);
5   **if** Match(N_a, N_s) > Match(N_a^{best}, N_s)
6         $N_a^{best} \leftarrow N_a$; $C \leftarrow G_a(L, x_a, y_a)$;
7 **return** C;

Table 2: *Pseudocode of the Algorithm*

The architecture of this algorithm is flexible; it is composed from several orthogonal components. We list these components as follows and discuss the corresponding design choices.

Pyramid: The pyramids are built from and reconstructed to images using the standard routines **BuildPyramid** and **ReconPyramid**. Various pyramids can be used for texture synthesis; examples are Gaussian pyramids [20], Laplacian pyramids [9], steerable pyramids [9, 22], and feature-based pyramids [4]. A Gaussian pyramid, for example, is built by successive filtering and downsampling operations, and each pyramid level, except for the highest resolution, is a blurred and decimated version of the original image. Reconstruction of Gaussian pyramids is trivial, since the image is available at the highest resolution pyramid level. These different pyramids give different trade-offs between spatial and frequency resolutions. In this paper, we choose to use the Gaussian pyramid for its simplicity and greater spatial localization (a detailed discussion of this issue can be found in [19]). However, other kinds of pyramids can be used instead.

Neighborhood: The neighborhood can have arbitrary size and shape; the only requirement is that it contains only valid pixels. A noncausal/symmetric neighborhood, for example, can be used by extending the original algorithm with two passes (Section 5.1).

Synthesis Ordering: A raster scan ordering is used in line 5 of the function **TextureSynthesis**. This, however, can also be extended. For example, a spiral ordering can be used for constrained texture synthesis (Section 5.1). The synthesis ordering should cooperate with the **BuildNeighborhood** so that the output neighborhoods contain only valid pixels.

Searching: An exhaustive searching procedure **FindBestMatch** is employed to determine the output pixel values. Because this is a standard process, various point searching algorithms can be used for acceleration. This will be discussed in detail in Section 4.

3 Synthesis Results

To test the effectiveness of our approach, we have run the algorithm on many different images from standard texture sets. Figure 8 shows examples using the MIT VisTex set [16], which contains real world textures photographed under natural lighting conditions. Additional texture synthesis results are available on our project website.

A visual comparison of our approach with several other algorithms is shown in Figure 9. Result (a) is generated by Heeger and Bergen's algorithm [9] using a steerable pyramid with 6 orientations. The algorithm captures certain random aspects of the texture but fails on the dominating grid-like structures. Result (b) is generated by De Bonet's approach [4] where we choose his randomness parameter to make the result look best. Though capable of capturing more structural patterns than (a), certain boundary artifacts are visible. This is because his approach characterizes textures by lower frequency pyramid levels only; therefore the lateral relationship between pixels at the same level is lost. Result (c) is generated by Efros and Leung's algorithm [6]. This technique is based on the Markov Random Field model and is capable of generating high quality textures. However, a direct application of their approach can produce non-tileable results.[2]

Result (d) is synthesized using our approach. It is tileable and the image quality is comparable with those synthesized directly from MRFs. It took about 8 minutes to generate using a 195 MHz R10000 processor. However, this is not the maximum possible speed achievable with this algorithm. In the next section, we describe modifications that accelerate the algorithm greatly.

4 Acceleration

Our deterministic synthesis procedure avoids the usual computational requirement for sampling from a MRF. However, the algorithm as described employs exhaustive searching, which makes it slow. Fortunately, acceleration is possible. This is achieved by considering neighborhoods $N(p)$ as points in a multiple dimensional space, and casting the neighborhood matching process as a nearest-point searching problem [17].

The nearest-point searching problem in multiple dimensions is stated as follows: given a set S of n points and a novel query point Q in a d-dimensional space, find a point in the set such that its distance from Q is lesser than, or equal to, the distance of Q from any other point in the set. Because a large number of such queries may need to be conducted over the same data set S, the computational cost can be reduced if we preprocess S to create a data structure that allows fast nearest-point queries. Many such data structures have been proposed, and we refer the reader to [17] for a more complete reference. However, most of these algorithms assume generic inputs and do not attempt to take advantage of any special structures they may have. Popat [20] observed that the set S of spatial neighborhoods from a texture can often be characterized well by

[2]Though not stated in the original paper [6], we have found that it is possible to extend their approach using multiresolution pyramids and a toroidal neighborhood to make tileable textures.

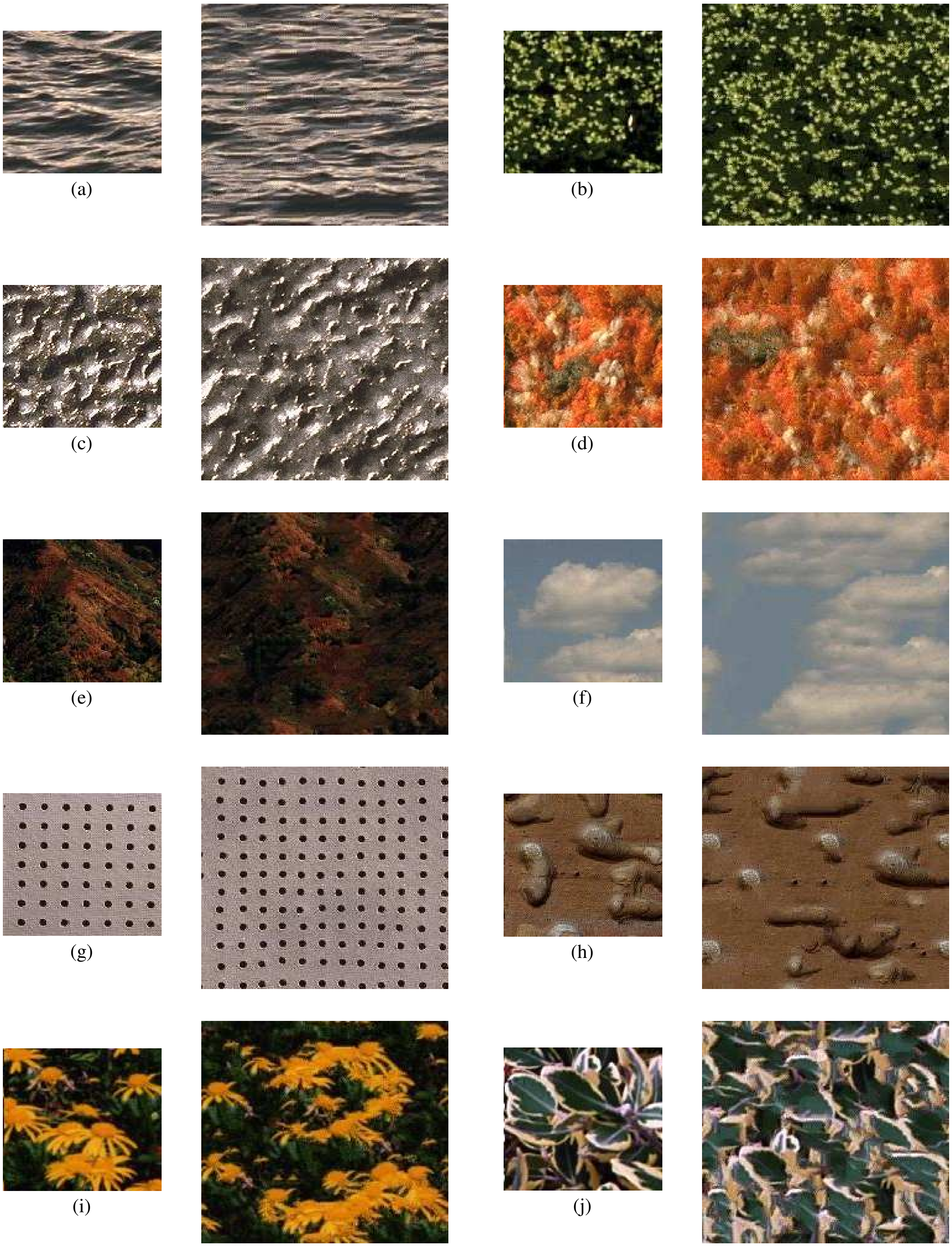

Figure 8: Texture synthesis results. The smaller patches (size 128x128) are the input textures, and to their right are synthesized results (size 200x200). Each texture is generated using a 4-level Gaussian pyramid, with neighborhood sizes {3x3,1}, {5x5,2}, {7x7,2}, {9x9,2}, respectively, from lower to higher resolutions. VisTex textures: (a) Water 0000 (b) Misc 0000 (c) Metal 0004 (d) Fabric 0015 (e) Terrain 0000 (f) Clouds 0000 (g) Tile 0007 (h) Stone 0002 (i) Flowers 0000 (j) Leaves 0009.

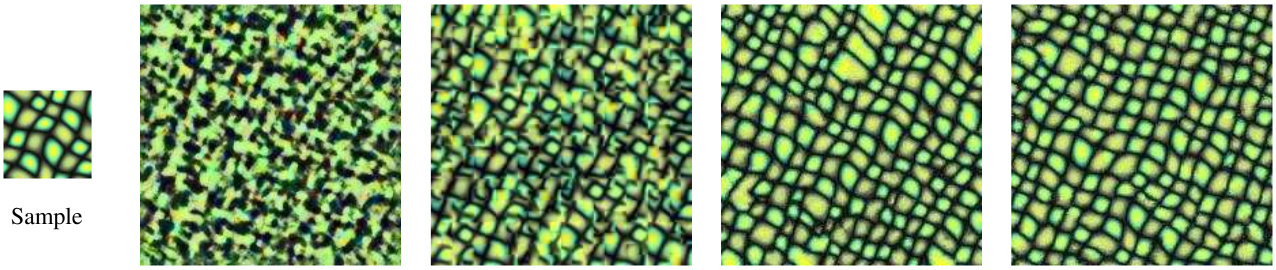

Sample

(a) (b) (c) (d)

Figure 9: *A comparison of texture synthesis results using different algorithms: (a) Heeger and Bergen's method [9] (b) De Bonet's method [4] (c) Efros and Leung's method [6] (d) Our method. Only Efros and Leung's algorithm produces results comparable with ours. However, our algorithm is two orders of magnitude faster than theirs (Section 4). The sample texture patch has size 64x64, and all the result images are of size 192x192. A 9x9 neighborhood is used for (c), and (d) is synthesized using the same parameters as indicated in the caption of Figure 8.*

a clustering probability model. Taking advantage of this clustering property, we propose to use tree-structured vector quantization (TSVQ, [7]) as the searching algorithm [25].

4.1 TSVQ Acceleration

Tree-structured vector quantization (TSVQ) is a common technique for data compression. It takes a set of training vectors as input, and generates a binary-tree-structured codebook. The first step is to compute the centroid of the set of training vectors and use it as the root level codeword. To find the children of this root, the centroid and a perturbed centroid are chosen as initial child codewords. A generalized Lloyd algorithm [7], consisting of alternations between centroid computation and nearest centroid partition, is then used to find the locally optimal codewords for the two children. The training vectors are divided into two groups based on these codewords and the algorithm recurses on each of the subtrees. This process terminates when the number of codewords exceeds a pre-selected size or the average coding error is below a certain threshold. The final codebook is the collection of the leaf level codewords.

The tree generated by TSVQ can be used as a data structure for efficient nearest-point queries. To find the nearest point of a given query vector, the tree is traversed from the root in a best-first ordering by comparing the query vector with the two children codewords, and then follows the one that has a closer codeword. This process is repeated for each visited node until a leaf node is reached. The best codeword is then returned as the codeword of that leaf node. Unlike full searching, the result codeword may not be the optimal one since only part of the tree is traversed. However, the result codeword is usually close to the optimal solution, and the computation is more efficient than full searching. If the tree is reasonably balanced (this can be enforced in the algorithm), a single search with codebook size $|S|$ can be achieved in time $O(log|S|)$, which is much faster than exhaustive searching with linear time complexity $O(|S|)$.

To use TSVQ in our synthesis algorithm, we simply collect the set of neighborhood pixels $N(p_i)$ for each input pixel and treat them as a vector of size equal to the number of pixels in $N(p_i)$. We use these vectors $\{N(p_i)\}$ from each $G_a(L)$ as the training data, and generate the corresponding tree structure codebooks $T(L)$. During the synthesis process, the (approximate) closest point for each $N(p)$ at $G_s(L)$ is found by doing a best-first traversal of $T(L)$. Because this tree traversal has time complexity $O(logN_L)$ (where N_L is the number of pixels of $G_a(L)$), the synthesis procedure can be executed very efficiently. Typical textures take seconds to generate; the exact timing depends on the input and output image sizes.

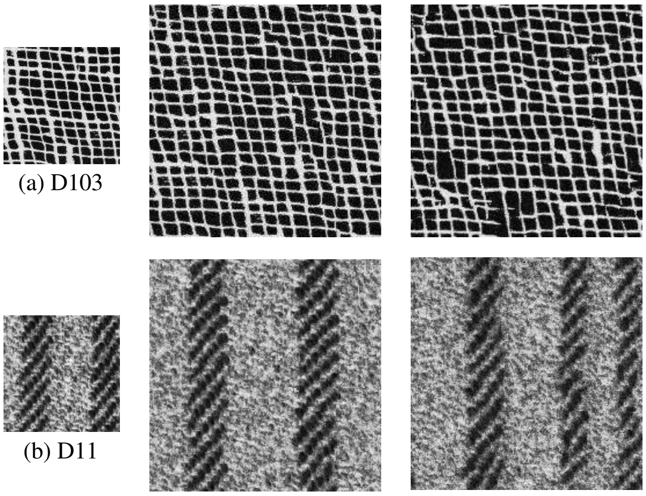

Figure 10: *Accelerated synthesis using TSVQ. The original Brodatz textures, with size 128x128, are shown in the left column. The results generated by exhaustive searching and TSVQ are shown in the middle and right columns, respectively. All generated images are of size 200x200. The average running time for exhaustive searching is 360 seconds. The average training time for TSVQ is 22 seconds and the average synthesis time is 7.5 seconds.*

4.2 Acceleration Results

An example comparing the results of exhaustive searching and TSVQ is shown in Figure 10. The original image sizes are 128x128 and the resulting image sizes are 200x200. The average running time for exhaustive searching is 360 seconds. The average training time for TSVQ is 22 seconds and the average synthesis time is 7.5 seconds. The code is implemented in C++ and the timings are measured on a 195MHz R10000 processor. As shown in Figure 10, results generated with TSVQ acceleration are roughly comparable in quality to those generated from the unaccelerated approach. In some cases, TSVQ will generate more blurry images. We fix this by allowing limited backtracking in the tree traversal so that more than one leaf node can be visited. The amount of backtracking can be used as a parameter which trades off between image quality and computation time. When the number of visited leaf nodes is equal to the codebook size, the result will be the same as the exhaustive searching case.

One disadvantage of TSVQ acceleration is the memory require-

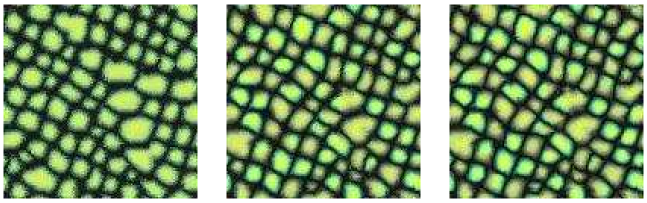

(a) (b) (c)

Figure 11: *TSVQ acceleration with different codebook sizes. The original image size is 64x64 and all these synthesized results are of size 128x128. The number of codewords in each case are (a) 64 (b) 512 (c) 4096 (all).*

Algorithm	Training Time	Synthesis Time
Efros and Leung	none	1941 seconds
Exhaustive Searching	none	503 seconds
TSVQ acceleration	12 seconds	12 seconds

Table 3: *A breakdown of running time for the textures shown in Figure 9. The first row shows the timing of Efros and Leung's algorithm. The second and third rows show the timing of our algorithm, using exhaustive searching and TSVQ acceleration, respectively. All the timings were measured using a 195 MHz R10000 processor.*

ment. Because an input pixel can appear in multiple neighborhoods, a full-sized TSVQ tree can consume $O(d * N)$ memory where d is the neighborhood size and N is the number of input image pixels. Fortunately, textures usually contain repeating structures; therefore we can use codebooks with fewer codewords than the input training set. Figure 11 shows textures generated by TSVQ with different codebook sizes. As expected the image quality improves when the codebook size increases. However, results generated with fewer codewords such as (b) look plausible compared with the full codebook result (c). In our experience we can use codebooks less than 10 percent the size of the original training data without noticeable degradation of quality of the synthesis results. To further reduce the expense of training, we can also train on a subset rather than the entire collection of input neighborhood vectors.

Table 3 shows a timing breakdown for generating the textures shown in Figure 9. Our unaccelerated algorithm took 503 seconds. The TSVQ accelerated algorithm took 12 seconds for training, and another 12 seconds for synthesis. In comparison, Efros and Leung's algorithm [6] took half an hour to generate the same texture (the time complexity of our approach over Efros and Leung's is $O(logN)/O(N)$ where N is the number of input image pixels). Because their algorithm uses a variable sized neighborhood it is difficult to accelerate. Our algorithm, on the other hand, uses a fixed neighborhood and can be directly accelerated by any point searching algorithm.

5 Applications

One of the chief advantages of our texture synthesis method is its low computational cost. This permits us to explore a variety of applications, in addition to the usual texture mapping for graphics, that were previously impractical. Presented here are constrained synthesis for image editing and temporal texture generation.

5.1 Constrained Texture Synthesis

Photographs, films and images often contain regions that are in some sense flawed. A flaw can be a scrambled region on a scanned photograph, scratches on an old film, wires or props in a movie film frame, or simply an undesirable object in an image. Since the processes causing these flaws are often irreversible, an algorithm that can fix these flaws is desirable. For example, Hirani and Totsuka [10] developed an interactive algorithm that finds translationally similar regions for noise removal. Often, the flawed portion is contained within a region of texture, and can be replaced by constrained texture synthesis [6, 11].

Texture replacement by constrained synthesis must satisfy two requirements: the synthesized region must look like the surrounding texture, and the boundary between the new and old regions must be invisible. Multiresolution blending [3] with another similar texture, shown in Figure 12 (b), will produce visible boundaries for structured textures. Better results can be obtained by applying our algorithm in Section 2 over the flawed regions, but discontinuities still appear at the right and bottom boundaries as shown in Figure 12 (c). These artifacts are caused by the causal neighborhood as well as the raster scan synthesis ordering.

To remove these boundary artifacts a noncausal (symmetric) neighborhood must be used. However, we have to modify the original algorithm so that only valid (already synthesized) pixels are contained within the symmetric neighborhoods; otherwise the algorithm will not generate valid results (Figure 5). This can be done with a two-pass extension of the original algorithm. Each pass is the same as the original multiresolution process, except that a different neighborhood is used. During the first pass, the neighborhood contains only pixels from the lower resolution pyramid levels. Because the synthesis progresses in a lower to higher resolution fashion, a symmetric neighborhood can be used without introducing invalid pixels. This pass uses the lower resolution information to "extrapolate" the higher resolution regions that need to be replaced. In the

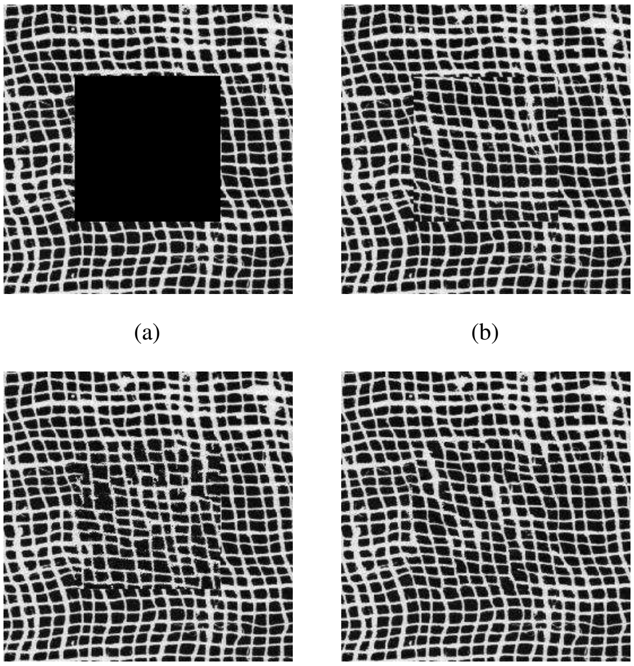

(a) (b) (c) (d)

Figure 12: *Constrained texture synthesis. (a) a texture containing a black region that needs to be filled in. (b) multiresolution blending [3] with another texture region will produce boundary artifacts. (c) A direct application of the algorithm in Section 2 will produce visible discontinuities at the right and bottom boundaries. (d) A much better result can be generated by using a modification of the algorithm with 2 passes.*

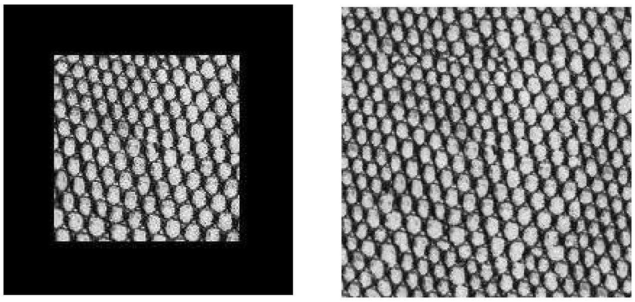

Original Result

Figure 13: *Image extrapolation of Brodatz texture D36. The original image is on the left and the synthesized result is on the right. The black region is filled in so that it looks consistent with the rest of the image.*

second pass, a symmetric neighborhood that contains pixels from both the current and lower resolutions is used. These two passes alternate for each level of the output pyramid. In the accelerated algorithm, the analysis phase is also modified so that two TSVQ trees corresponding to these two kinds of neighborhoods are built for each level of the input pyramid. Finally, we also modify the synthesis ordering in the following way: instead of the usual raster-scan ordering, pixels in the filled regions are assigned in a spiral fashion. For example, the hole in Figure 12 (a) is replaced from outside to inside from the surrounding region until every pixel is assigned (Figure 12 (d)). This spiral synthesis ordering removes the directional bias which causes the boundary discontinuities (as in Figure 12 (c)).

With a slight change of the synthesis ordering, the algorithm can be applied to other applications, such as the image extrapolation shown in Figure 13. The algorithm could also be extended as an interactive tool for image editing or denoising [15].

5.2 Temporal Texture Synthesis

The low cost of our accelerated algorithm enables us to consider synthesizing textures of dimension greater than two. An example of 3D texture is a temporal texture. Temporal textures are motions with indeterminate extent both in space and time. They can describe a wide variety of natural phenomena such as fire, smoke, and fluid motions. Since realistic motion synthesis is one of the major goals of computer graphics, a technique that can synthesize temporal textures would be useful. Most existing algorithms model temporal textures by direct simulation; examples include fluid, gas, and fire [23]. Direct simulations, however, are often expensive and only suitable for specific kinds of textures; therefore an algorithm that can model general motion textures would be advantageous [24].

Temporal textures consist of 3D spatial-temporal volume of motion data. If the motion data is local and stationary both in space and time, the texture can be synthesized by a 3D extension of our algorithm. This extension can be simply done by replacing various 2D entities in the original algorithm, such as images, pyramids, and neighborhoods, with their 3D counterparts. For example, the two Gaussian pyramids are constructed by filtering and downsampling from 3D volumetric data; the neighborhoods contain local pixels in both the spatial and temporal dimension. The synthesis progresses from lower to higher resolutions, and within each resolution the output is synthesized slice by slice along the time domain.

Figure 14 shows synthesis results of several typical temporal textures: fire, smoke, and ocean waves (animations available on our webpage). The resulting sequences capture the flavor of the original motions, and tile both spatially and temporally. This technique is also efficient. Accelerated by TSVQ, each result frame took about 20 seconds to synthesize. Currently all the textures are generated automatically; we plan to extend the algorithm to allow more explicit user controls (such as the distribution and intensity of the fire and smoke).

6 Conclusions and Future Work

Textures are important for a wide variety of applications in computer graphics and image processing. On the other hand, they are hard to synthesize. The goal of this paper is to provide a practical tool for efficiently synthesizing a broad range of textures. Inspired by Markov Random Field methods, our algorithm is general: a wide variety of textures can be synthesized without any knowledge of their physical formation processes. The algorithm is also efficient: by a proper acceleration using TSVQ, typical textures can be generated within seconds on current PCs and workstations. The algorithm is also easy to use: only an example texture patch is required.

The basic version of our algorithm (Section 2) relates to an earlier work by Popat and Picard [20] in that a causal neighborhood and raster scan ordering are used for texture synthesis. However, instead of constructing explicit probability models, our algorithm uses deterministic searching. This approach shares the simplicity of Efros and Leung [6], but uses fix-sized neighborhoods which allow TSVQ acceleration. The fact that such a simple approach works well on many different textures implies that there may be computational redundancies in other texture synthesis techniques. This algorithm shares some of the same limitations as Markov Random Field approaches: in particular, only local and stationary phenomena can be represented. Other visual cues such as 3D shape, depth, lighting, or reflection can not be captured by this simple model.

Aside from constrained synthesis and temporal textures, numerous applications of our approach are possible. Other potential applications/extensions are:

Multidimensional texture: The notion of texture extends naturally to multi-dimensional data. One example was presented in this paper - motion sequences. The same technique can also be directly applied to solid textures or animated solid texture synthesis. We are also trying to extend our algorithm for generating structured solid textures from 2D views [9].

Texture compression/decompression: Textures usually contain repeating patterns and high frequency information; therefore they are not well compressed by transform-based techniques such as JPEG. However, codebook-based compression techniques work well on textures [1]. This suggests that textures might be compressable by our synthesis technique. Compression would consist of building a codebook, but unlike [1], no code indices would be generated; only the codebook would be transmitted and the compression ratio is controlled by the number of codewords. Decompression would consist of texture synthesis. This decompression step, if accelerated one more order of magnitude over our current software implementation, could be usable for real time texture mapping. The advantage of this approach over [1] is much greater compression, since only the codebook is transmitted.

Motion synthesis/editing: Some motions can be efficiently modeled as spatial-temporal textures. Others, such as animal or human motion, are too highly structured for such a direct approach. However, it might be possible to encode their motion as joint angles, and then apply texture analysis-synthesis to the resulting 1D temporal motion signals.

Modeling geometric details: Models scanned from real world objects often contain texture-like geometric details, making the

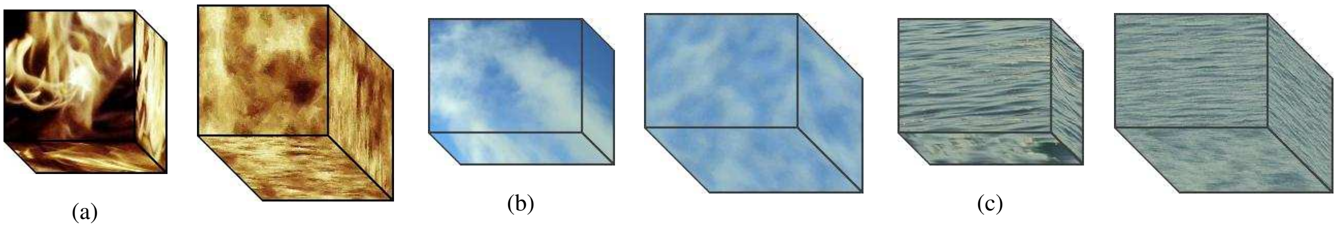

(a) (b) (c)

Figure 14: *Temporal texture synthesis results. (a) fire (b) smoke (c) ocean waves. In each pair of images, the spatial-temporal volume of the original motion sequence is shown on the left, and the corresponding synthesis result is shown on the right. A 3-level Gaussian pyramid, with neighborhood sizes {5x5x5,2}, {3x3x3,2}, {1x1x1,1}, are used for synthesis. The original motion sequences contain 32 frames, and the synthesis results contain 64 frames. The individual frame sizes are (a) 128x128 (b) 150x112 (c) 150x112. Accelerated by TSVQ, the training times are (a) 1875 (b) 2155 (c) 2131 seconds and the synthesis times per frame are (a) 19.78 (b) 18.78 (c) 20.08 seconds. To save memory, we use only a random 10 percent of the input neighborhood vectors to build the (full) codebooks.*

models expensive to store, transmit or manipulate. These geometric details can be represented as displacement maps over a smoother surface representation [13]. The resulting displacement maps should be compressable/decompressable as 2D textures using our technique. Taking this idea further, missing geometric details, a common problem in many scanning situations [14], could be filled in using our constrained texture synthesis technique.

Direct synthesis over meshes: Mapping textures onto irregular 3D meshes by projection often causes distortions [21]. These distortions can sometimes be fixed by establishing suitable parameterization of the mesh, but a more direct approach would be to synthesize the texture directly over the mesh. In principle, this can be done using our technique. However, this will require extending ordinary signal processing operations such as filtering and downsampling to irregular 3D meshes.

Acknowledgments

We would like to thank Kris Popat and Alyosha Efros for answering questions about their texture synthesis works, Phil Hubbard for his help on the writing of the paper, and the anonymous reviewers for their comments. The texture thumbnail shown in Figure 1 was acquired from Jeremy De Bonet's webpage. Special thanks to members of the Stanford Graphics Group. This research was supported by Intel, Interval, and Sony under the Stanford Immersive Television Project.

References

[1] A. C. Beers, M. Agrawala, and N. Chaddha. Rendering from compressed textures. *Proceedings of SIGGRAPH 96*, pages 373–378, August 1996.

[2] P. Brodatz. *Textures: A Photographic Album for Artists and Designers*. Dover, New York, 1966.

[3] P. J. Burt and E. H. Adelson. A multiresolution spline with application to image mosaics. *ACM Transactions on Graphics*, 2(4):217–236, Oct. 1983.

[4] J. S. De Bonet. Multiresolution sampling procedure for analysis and synthesis of texture images. In T. Whitted, editor, *SIGGRAPH 97 Conference Proceedings*, Annual Conference Series, pages 361–368. ACM SIGGRAPH, Addison Wesley, Aug. 1997.

[5] J. Dorsey, A. Edelman, J. Legakis, H. W. Jensen, and H. K. Pedersen. Modeling and rendering of weathered stone. *Proceedings of SIGGRAPH 99*, pages 225–234, August 1999.

[6] A. Efros and T. Leung. Texture synthesis by non-parametric sampling. In *International Conference on Computer Vision*, volume 2, pages 1033–8, Sep 1999.

[7] A. Gersho and R. M. Gray. *Vector Quantization and Signal Compression*. Kluwer Academic Publishers, 1992.

[8] R. Haralick. Statistical image texture analysis. In *Handbook of Pattern Recognition and Image Processing*, volume 86, pages 247–279. Academic Press, 1986.

[9] D. J. Heeger and J. R. Bergen. Pyramid-Based texture analysis/synthesis. In R. Cook, editor, *SIGGRAPH 95 Conference Proceedings*, Annual Conference Series, pages 229–238. ACM SIGGRAPH, Addison Wesley, Aug. 1995.

[10] A. N. Hirani and T. Totsuka. Combining frequency and spatial domain information for fast interactive image noise removal. *Computer Graphics*, 30(Annual Conference Series):269–276, 1996.

[11] H. Igehy and L. Pereira. Image replacement through texture synthesis. In *International Conference on Image Processing*, volume 3, pages 186–189, Oct 1997.

[12] H. Iversen and T. Lonnestad. An evaluation of stochastic models for analysis and synthesis of gray scale texture. *Pattern Recognition Letters*, 15:575–585, 1994.

[13] V. Krishnamurthy and M. Levoy. Fitting smooth surfaces to dense polygon meshes. *Proceedings of SIGGRAPH 96*, pages 313–324, August 1996. ISBN 0-201-94800-1. Held in New Orleans, Louisiana.

[14] M. Levoy, K. Pulli, B. Curless, S. Rusinkiewicz, D. Koller, L. Pereira, M. Ginzton, S. Anderson, J. Davis, J. Ginsberg, J. Shade, and D. Fulk. The Digital Michelangelo Project: 3D scanning of large statues. To appear in Proceedings of SIGGRAPH 2000.

[15] T. Malzbender and S. Spach. A context sensitive texture nib. In *Proceedings of Computer Graphics International*, pages 151–163, June 1993.

[16] MIT Media Lab. Vision texture. http://www-white.media.mit.edu/vismod/-imagery/VisionTexture/vistex.html.

[17] S. Nene and S. Nayar. A simple algorithm for nearest neighbor search in high dimensions. *IEEE Transactions on Pattern Analysis and Machine Intelligence*, 19:989–1003, 1997.

[18] R. Paget and I. Longstaff. Texture synthesis via a noncausal nonparametric multiscale Markov random field. *IEEE Transactions on Image Processing*, 7(6):925–931, June 1998.

[19] A. C. Popat. *Conjoint Probabilistic Subband Modeling*. PhD thesis, Massachusetts Institute of Technology, 1997.

[20] K. Popat and R. Picard. Novel cluster-based probability model for texture synthesis, classification, and compression. In *Visual Communications and Image Processing*, pages 756–68, 1993.

[21] M. Segal, C. Korobkin, R. van Widenfelt, J. Foran, and P. E. Haeberli. Fast shadows and lighting effects using texture mapping. *Computer Graphics (Proceedings of SIGGRAPH 92)*, 26(2):249–252, July 1992.

[22] E. Simoncelli and J. Portilla. Texture characterization via joint statistics of wavelet coefficient magnitudes. In *Fifth International Conference on Image Processing*, volume 1, pages 62–66, Oct. 1998.

[23] J. Stam and E. Fiume. Depicting fire and other gaseous phenomena using diffusion processes. *Proceedings of SIGGRAPH 95*, pages 129–136, August 1995.

[24] M. Szummer and R. W. Picard. Temporal texture modeling. In *International Conference on Image Processing*, volume 3, pages 823–6, Sep 1996.

[25] L. Wei. Deterministic texture analysis and synthesis using tree structure vector quantization. In *XII Brazilian Symposium on Computer Graphics and Image Processing*, pages 207–213, October 1999.

[26] A. Witkin and M. Kass. Reaction-diffusion textures. In T. W. Sederberg, editor, *Computer Graphics (SIGGRAPH '91 Proceedings)*, volume 25, pages 299–308, July 1991.

[27] S. P. Worley. A cellular texture basis function. In H. Rushmeier, editor, *SIGGRAPH 96 Conference Proceedings*, Annual Conference Series, pages 291–294. ACM SIGGRAPH, Addison Wesley, Aug. 1996.

[28] S. Zhu, Y. Wu, and D. Mumford. Filters, random fields and maximun entropy (FRAME) - towards a unified theory for texture modeling. *International Journal of Computer Vision*, 27(2):107–126, 1998.